

# On the Inductive Bias of a CNN for Orthogonal Patterns Distributions

Alon Brutzkus<sup>1</sup> Amir Globerson<sup>1</sup>

## Abstract

Training overparameterized convolutional neural networks with gradient based methods is the most successful learning method for image classification. However, its theoretical properties are far from understood even for very simple learning tasks. In this work, we consider a simplified image classification task where images contain orthogonal patches and are learned with a 3-layer overparameterized convolutional network and stochastic gradient descent. We empirically identify a novel phenomenon where the dot-product between the learned pattern detectors and their detected patterns are governed by the pattern statistics in the training set. We call this phenomenon Pattern Statistics Inductive Bias (PSI) and prove that PSI holds for a simple setup with two points in the training set. Furthermore, we prove that if PSI holds, stochastic gradient descent has sample complexity  $O(d^2 \log(d))$  where  $d$  is the filter dimension. In contrast, we show a VC dimension lower bound in our setting which is exponential in  $d$ . Taken together, our results provide strong evidence that PSI is a unique inductive bias of stochastic gradient descent, that guarantees good generalization properties.

## 1. Introduction

Convolutional neural networks (CNNs) have achieved remarkable performance in various computer vision tasks (Krizhevsky et al., 2012; Xu et al., 2015; Taigman et al., 2014). In practice, these networks typically have more parameters than training points (i.e., are overparameterized), and are trained with gradient based methods. Despite non-convexity and the potential problem of overfitting, these algorithms find solutions with low test error. It is still largely unknown why such simple optimization algorithms have outstanding test performance for learning overparameterized

<sup>1</sup>The Blavatnik School of Computer Science, Tel Aviv University. Correspondence to: Alon Brutzkus <alon-brutzkus@mail.tau.ac.il>.

Preliminary work.

convolutional networks.

Recently, there have been major efforts to provide theoretical guarantees for overparameterized neural networks. However, these results do not provide guarantees in practical settings even for very simple learning tasks. Current results either hold for the Neural Tangent Kernel regime (NTK) where neural network dynamics are approximately linear, or do not provide good generalization guarantees for datasets of practical size. However, NTK is not an accurate model of neural networks in practice (Yehudai & Shamir, 2019; Bai & Lee, 2019; Woodworth et al., 2019) and empirically small datasets suffice for good generalization. The difficulty is that even for very simple tasks the optimization problem is non-convex and obtaining practical generalization guarantees is a major challenge.

Therefore, to fully understand overparameterized convolutional neural networks it is necessary to first understand simple settings which are amenable to theoretical and empirical analysis. Towards this goal, we analyze a simplified pattern recognition task where all patterns in the images are orthogonal and the classification is binary. We consider learning a 3-layer overparameterized convolutional neural network with stochastic gradient descent (SGD). We take a unique approach that combines both a novel empirical insight and theoretical guarantees which pinpoint the inductive bias of overparameterized convolutional neural networks in our setting and show why SGD generalizes well.

Empirically, we identify a novel property of the solutions found by SGD, in which the statistics of patterns in the training data govern the magnitude of the dot-product between learned pattern detectors and their detected patterns. Specifically, patterns that appear almost exclusively in one of the classes will have a large dot-product with the channels that detect them. On the other hand, patterns that appear roughly equally in both classes, will have a low dot-product with their detecting channels. We formally define this ‘‘Pattern Statistics Inductive Bias’’ condition (PSI) and provide empirical evidence that PSI holds across a large number of settings. We also prove that SGD indeed satisfies PSI in a simple setup of two points in the training set.

Under the assumption that PSI holds, we analyze the sample complexity of SGD and prove that it is at most  $O(d^2 \log d)$ , where  $d$  is the filter dimension. This is a very good sample

complexity since the filter dimension is usually small in practice. Furthermore, it is independent of the number of hidden units in the network. In contrast, we show that the VC dimension of the class of functions we consider is exponential in  $d$ , and thus there exist other learning algorithms (not SGD) that will have exponential sample complexity. Together, these results provide firm evidence that even though SGD can in principle overfit, it is nonetheless biased towards solutions which are determined by the statistics of the patterns in the training set and consequently it has very good generalization performance. Our results suggest that PSI is a fundamental property of gradient descent and we believe that it can pave the way for analyzing and understanding other settings of overparameterized CNNs.

## 2. Related Work

Several recent works have studied the inductive bias of gradient based methods learning CNNs. Numerous works show that under simplified assumptions, e.g., linearly separable data or linear networks, gradient methods are biased towards low norm or low rank solutions (Ji & Telgarsky, 2019; 2018; Soudry et al., 2018; Brutzkus et al., 2018; Arora et al., 2019a; Nacson et al., 2019; Lyu & Li, 2019; Wei et al., 2019). Other works study the inductive bias via the NTK approximation (Du et al., 2019; 2018c; Arora et al., 2019b; Fiat et al., 2019). We present a novel view of the inductive bias of SGD that is complimentary to these approaches.

Yu et al. (2019) study a pattern classification problem similar to ours. However, their analysis holds for an unbounded hinge loss which is not used in practice. Furthermore, their sample complexity depends on the network size, and thus does not explain why large networks do not overfit. Other works have studied learning under certain ground truth distributions. For example, Brutzkus & Globerson (2019) study a simple extension of the XOR problem, showing that overparameterized CNNs generalize better than smaller CNNs. Single-channel CNNs are analyzed in (Du et al., 2018b;a; Brutzkus & Globerson, 2017).

## 3. The Orthogonal Patterns Problem

**Data Generating Distribution:** We consider a learning problem that captures a key property of visual classification. Many visual classes are characterized by the existence of certain patterns in the data. For example an 8 will typically contain an x like pattern somewhere in the image. Here we consider an abstraction of this behavior where images consist of a set of patterns. Furthermore, each class is characterized by a pattern that appears exclusively in it (see Fig. 1). We define this formally below.

Let  $\mathcal{P}$  be a set of orthogonal vectors in  $\mathbb{R}^d$ , where  $|\mathcal{P}| \leq d$ . For simplicity, we assume that  $\|p\|_2 = 1$  for all  $p \in \mathcal{P}$ . We

consider input vectors  $\mathbf{x}$  with  $n$  patterns of dimension  $d$ . Formally,  $\mathbf{x} = (\mathbf{x}[1], \dots, \mathbf{x}[n]) \in \mathbb{R}^{nd}$  where  $\mathbf{x}[i] \in \mathcal{P}$  is the  $i$ th pattern of  $\mathbf{x}$  and  $n < d$ . For a pattern  $p \in \mathcal{P}$  we denote  $p \in \mathbf{x}$  if  $\mathbf{x}$  contains the pattern  $p$ .<sup>1</sup> Let  $\mathcal{P}_x = \{p \in \mathbf{x} \mid p \in \mathcal{P}\}$ . We define  $\mathcal{P} = \mathcal{P}_+ \cup \mathcal{P}_- \cup \mathcal{P}_J$ , where the union is disjoint,  $\mathcal{P}_+$  is the set of positive patterns,  $\mathcal{P}_-$  the set of negative patterns and  $\mathcal{P}_J$  is the set of joint patterns.

For simplicity, in this work we consider the case where  $|\mathcal{P}_+| = |\mathcal{P}_-| = 1$ . We denote,  $\mathcal{P} = \{p_1, p_2, \dots, p_{|\mathcal{P}|}\}$ ,  $\mathcal{P}_+ = \{p_1\}$  and  $\mathcal{P}_- = \{p_2\}$ . For convenience, we also refer to a set of patterns  $A$  as a set of the indices of the patterns. For example, we denote  $i \in A$  if  $p_i \in A$ .

We consider distributions  $\mathcal{D}$  over  $(\mathbf{x}, y) \in \mathbb{R}^{nd} \times \{\pm 1\}$  with the following properties:

1.  $\mathbb{P}(y = 1) = \mathbb{P}(y = -1) = \frac{1}{2}$ .
2. Given  $y = 1$ , a vector  $\mathbf{x}$  is sampled as follows. Choose the positive pattern  $p_1 \in \mathcal{P}_+$  and randomly choose a set of  $n - 1$  patterns from  $\mathcal{P}_J$ . Denote this set of  $n$  chosen patterns by  $A$ . Set  $\mathbf{x}$  be some  $\mathbf{x}$  such that  $\mathcal{P}_x = A$ , where the location of each pattern in  $\mathbf{x}$  is chosen arbitrarily.<sup>2</sup> For example, if  $n = 3$  and the  $n - 1$  patterns are  $p_3, p_7$  this can result in samples such as  $([p_1, p_7, p_3], 1)$  or  $([p_3, p_1, p_7], 1)$ .
3. Similarly given  $y = -1$ , choose the negative pattern  $p_2 \in \mathcal{P}_-$  and continue as for the positive pattern above.

Fig. 1 shows an example of samples generated using the above procedure. We note that any distribution which satisfies the above is linearly separable. In Sec. 7 we will introduce several distributions that satisfy the above conditions. They will differ in the sampling procedure of joint patterns.

**Neural Architecture:** We are interested in neural architectures that can learn pattern detection problems such as the one above. A natural model in this context is a 3-layer network with a convolutional layer, followed by ReLU, max pooling and a fully-connected layer. Each channel in the first layer can be thought of as a detector for a given pattern. We say that a detector detects pattern  $p \in \mathcal{P}$ , if  $p$  has the largest dot product with the detector among all patterns in  $\mathcal{P}$  and this dot product is positive. For simplicity we fix the weights on the last linear layer to values  $\pm 1$ .

Let  $2k$  denote the number of channels. We partition the channels into two sets:  $\mathbf{w}^{(1)}, \dots, \mathbf{w}^{(k)}$  and  $\mathbf{u}^{(1)}, \dots, \mathbf{u}^{(k)}$ . These will have weights of  $+1$  and  $-1$  in the output respec-

<sup>1</sup>We say that  $\mathbf{x}$  contains  $p$  if there exists  $j$  such that  $\mathbf{x}[j] = p$ .

<sup>2</sup>We will see that the order of the patterns does not matter, because the convolutional network is invariant to this order.

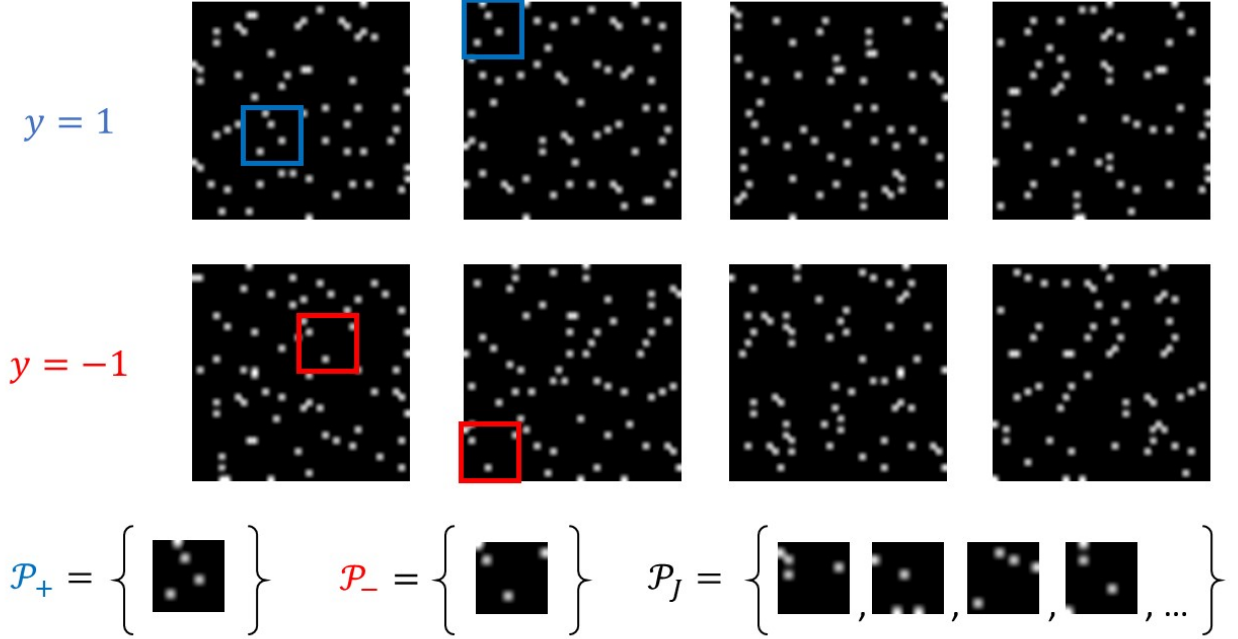


Figure 1. Example of points in orthogonal patterns distributions. Here there are 25 possible orthogonal patterns ( $|\mathcal{P}| = 25$ ) and each pattern is a  $10 \times 10$  image patch and thus  $d = 100$ . The number of patterns in each image is  $n = 16$ . The image consists of 4 rows of 4 patches each. The positive examples contain the pattern in  $\mathcal{P}_+$ . The negative examples contain the pattern in  $\mathcal{P}_-$ . In the two leftmost images of each class, the corresponding pattern is shown. All other patterns in an image are from  $\mathcal{P}_J$ . This example illustrates that even though we consider simplified distributions, it can be difficult to manually find the discriminating patterns of each class and classify the images.

tively. Finally, let  $W \in \mathbb{R}^{2k \times 2}$  be the weight matrix whose rows are  $\mathbf{w}^{(i)}$  followed by  $\mathbf{u}^{(i)}$ .

For an input  $\mathbf{x} = (\mathbf{x}[1], \dots, \mathbf{x}[n]) \in \mathbb{R}^{nd}$  where  $\mathbf{x}[i] \in \mathbb{R}^d$ , the output of the network, denoted by  $N_W^k(\mathbf{x})$  is given by:

$$\sum_{i=1}^k \left[ \max_j \{ \sigma(\mathbf{w}^{(i)} \cdot \mathbf{x}[j]) \} - \max_j \{ \sigma(\mathbf{u}^{(i)} \cdot \mathbf{x}[j]) \} \right] \quad (1)$$

where  $\sigma(x) = \max\{0, x\}$  is the ReLU activation applied element-wise. Let  $\mathcal{H}$  denote the class of all networks  $N_W^k$  in Eq. 1, with any value of  $k > 0$ . Finally, we note that  $\mathcal{H}$  can perfectly fit the distribution  $\mathcal{D}$  above, by setting  $k = 1$ ,  $\mathbf{w}^{(1)} = \mathbf{p}_1$  and  $\mathbf{u}^{(1)} = \mathbf{p}_2$ . Therefore, for  $k > 1$  the network is overparameterized.

**Training Algorithm:** Let  $S$  be a training set with  $m$  IID samples from  $\mathcal{D}$ . We consider minimizing the hinge loss:

$$\ell(W) = \frac{1}{m} \sum_{(\mathbf{x}_i, y_i) \in S} \max\{1 - y_i N_W^k(\mathbf{x}_i), 0\} \quad (2)$$

For optimization, we use SGD with constant learning rate  $\eta$ . The parameters  $W$  are initialized as IID Gaussians with

zero mean and standard deviation  $\sigma_g$ . Let  $W_t$  be the weight matrix at iteration  $t$  of SGD. Similarly let  $\mathbf{w}_t^{(i)}, \mathbf{u}_t^{(i)}$  be the corresponding vectors at iteration  $t$ .

**Detection Ratios:** We now define the notion of detection ratios, that will be key to our analysis. Towards this end, we define the following:

$$\begin{aligned} \mathcal{W}^+(i) &= \left\{ j \mid \arg \max_{l \in \mathcal{P}_J \cup \mathcal{P}_+} \mathbf{w}^{(j)} \cdot \mathbf{p}_l = i, \mathbf{w}^{(j)} \cdot \mathbf{p}_i > 0 \right\} \\ \mathcal{U}^+(i) &= \left\{ j \mid \arg \max_{l \in \mathcal{P}_J \cup \mathcal{P}_+} \mathbf{u}^{(j)} \cdot \mathbf{p}_l = i, \mathbf{u}^{(j)} \cdot \mathbf{p}_i > 0 \right\} \end{aligned} \quad (3)$$

and

$$M_{\mathbf{w}}^+(i) = \sum_{j \in \mathcal{W}^+(i)} \mathbf{w}^{(j)} \cdot \mathbf{p}_i, M_{\mathbf{u}}^+(i) = \sum_{j \in \mathcal{U}^+(i)} \mathbf{u}^{(j)} \cdot \mathbf{p}_i \quad (4)$$

The quantity  $M_{\mathbf{w}}^+(i)$  is the sum of the dot product between pattern  $\mathbf{p}_i$  and its detector  $\mathbf{w}^{(j)}$ , over all detectors  $\mathbf{w}^{(j)}$  of  $\mathbf{p}_i$  ( $M_{\mathbf{u}}^+(i)$  is similar but with detectors  $\mathbf{u}^{(j)}$ ).

For all  $\mathbf{p}_i \in \mathcal{P}_+ \cup \mathcal{P}_J$  we say that  $\frac{M_{\mathbf{u}}^+(i)}{M_{\mathbf{u}}^+(1)}$  are *positive detection ratios*.

We can now derive the following key observation for any positive point  $\mathbf{x}^+$ :

$$\begin{aligned} N_W^k(\mathbf{x}^+) &\geq M_{\mathbf{w}}^+(1) - \sum_{\mathbf{p}_i \in \mathcal{P}_J \cup \mathcal{P}_+} M_{\mathbf{u}}^+(i) \\ &= M_{\mathbf{w}}^+(1) \left( 1 - \sum_{\mathbf{p}_i \in \mathcal{P}_J \cup \mathcal{P}_+} \frac{M_{\mathbf{u}}^+(i)}{M_{\mathbf{w}}^+(1)} \right) \quad (5) \end{aligned}$$

Notice that if all positive detection ratios are small, then the positive point is classified correctly. We will show that for SGD, the magnitude of the detection ratios are governed by the statistics of the patterns in the training set, which will imply our generalization result.

Similarly, we define the following:

$$\begin{aligned} \mathcal{W}^-(i) &= \left\{ j \mid \arg \max_{l \in \mathcal{P}_J \cup \mathcal{P}_-} \mathbf{w}^{(j)} \cdot \mathbf{p}_l = i, \mathbf{w}^{(j)} \cdot \mathbf{p}_i > 0 \right\} \\ \mathcal{U}^-(i) &= \left\{ j \mid \arg \max_{l \in \mathcal{P}_J \cup \mathcal{P}_-} \mathbf{u}^{(j)} \cdot \mathbf{p}_l = i, \mathbf{u}^{(j)} \cdot \mathbf{p}_i > 0 \right\} \quad (6) \end{aligned}$$

and

$$M_{\mathbf{w}}^-(i) = \sum_{j \in \mathcal{W}^-(i)} \mathbf{w}^{(j)} \cdot \mathbf{p}_i, \quad M_{\mathbf{u}}^-(i) = \sum_{j \in \mathcal{U}^-(i)} \mathbf{u}^{(j)} \cdot \mathbf{p}_i \quad (7)$$

Now, for all  $\mathbf{p}_i \in \mathcal{P}_- \cup \mathcal{P}_J$  we say that  $\frac{M_{\mathbf{w}}^-(i)}{M_{\mathbf{w}}^-(2)}$  are *negative detection ratios*. Then, for any negative point  $\mathbf{x}^-$  we have:

$$-N_W^k(\mathbf{x}^-) \geq M_{\mathbf{u}}^-(2) \left( 1 - \sum_{\mathbf{p}_i \in \mathcal{P}_J \cup \mathcal{P}_-} \frac{M_{\mathbf{w}}^-(i)}{M_{\mathbf{w}}^-(2)} \right) \quad (8)$$

which similarly shows that if the negative detection ratios are small, then all negative points are classified correctly. In the rest of the paper, we refer to both positive and negative detection ratios as detection ratios.

**Empirical Pattern Bias:** In a given training set, patterns will appear in both positive and negative labels. The following measure captures how well-balanced are the patterns between the labels. For any pattern  $\mathbf{p}_i \in \mathcal{P}$ , define the following statistic of the training set:

$$s_i = \frac{\sum_{(\mathbf{x}_j, y_j) \in S} y_j \mathbb{1}\{\mathbf{p}_i \in \mathbf{x}_j\}}{m} \quad (9)$$

The detection ratios define quantities of the learned model. On the other hand, Eq. 9 is a quantity of the sampled training set. In the next section, we define the PSI property, which specifies how these two measures should be related to guarantee good generalization for the learned model.

## 4. Pattern Statistics Inductive Bias

The inductive bias of a learning algorithm refers to how the algorithm chooses among all models that fit the data equally well. For example, an SVM algorithm has an inductive bias towards low norm. Indeed, as noted in [Zhang et al. \(2017\)](#), understanding the success of deep learning requires understanding the inductive bias of the learning algorithms used to learn networks, and in particular SGD.

In what follows, we define a certain inductive bias of an algorithm, which we refer to as the Patterns Statistics Inductive Bias (PSI) property. The PSI property states a simple relation between the relative frequency of patterns  $s_i$  (see Eq. 9) and the detection ratios. We begin by providing the formal definition of PSI, and then provide further intuition. For the definition, we let  $\mathcal{A}$  be any learning algorithm which given a training set  $S$  returns a network  $\mathcal{A}(S)$  as in Eq. 1.

**Definition 4.1.** *We say that a learning algorithm  $\mathcal{A}$  satisfies the Patterns Statistics Inductive Bias condition with constants  $b, c, \delta > 0$  (( $b, c, \delta$ )-PSI) if the following holds. For any  $m \geq d^2$ , <sup>3</sup> with probability at least  $1 - \delta$  over the randomization of  $\mathcal{A}$  and training set  $S$  of size  $m$ ,  $\mathcal{A}(S)$  satisfies the following:*

1. For all  $i \in \mathcal{P}_J \cup \mathcal{P}_+$ :

$$\frac{M_{\mathbf{u}}^+(i)}{M_{\mathbf{u}}^+(1)} \leq b \max\left(-\frac{s_i}{s_1}, 0\right) + \frac{c}{\sqrt{m}}$$

2. For all  $i \in \mathcal{P}_J \cup \mathcal{P}_-$ :

$$\frac{M_{\mathbf{w}}^-(i)}{M_{\mathbf{w}}^-(2)} \leq b \max\left(-\frac{s_i}{s_2}, 0\right) + \frac{c}{\sqrt{m}}$$

We next provide some informal intuition as to why SGD updates may lead to PSI (in Sec. 8 we provide a proof of this for a restricted setting).

We will consider updates made by gradient descent (full batch SGD). Define  $\mathcal{W}_t^+(i)$  to be the set  $\mathcal{W}^+(i)$  with weight vectors  $\mathbf{w}_t^{(j)}$  instead of  $\mathbf{w}^{(j)}$ . Similarly, define  $\mathcal{U}_t^+(i)$ ,  $\mathcal{W}_t^-(i)$  and  $\mathcal{U}_t^-(i)$ . Throughout the discussion below, we assume that these sets have roughly the same size. This holds with high probability at initialization for a sufficiently large network. Furthermore, in Section 8, we show that it holds during training in the case of two training points.

Note that the gradient is a sum of updates, one for each point in the training set. First assume that  $j \in \mathcal{W}_t^+(1)$ . Then by the gradient update, the value  $\frac{\eta}{m} \mathbf{p}_1$  is added to  $\mathbf{w}_t^{(j)}$  for all positive points that have non-zero hinge loss. The value  $-\frac{\eta}{m} \mathbf{p}_i$  is also added for a few  $\mathbf{p}_i \in \mathcal{P}_- \cup \mathcal{P}_J$  and a subset of the negative points ( $i$  depends on the specific negative

<sup>3</sup>We chose  $d^2$  for simplicity, it can be replaced by any constant.

point). In the next iteration, it holds that  $j \in \mathcal{W}_{t+1}^+(1)$  and the updates continue similarly. Overall, we see that  $\mathbf{w}_t^{(j)} \cdot \mathbf{p}_1$  increases in each iteration and should be large after a few iterations. Therefore,  $M_{\mathbf{w}}^+(1)$  should be large.

Now assume that  $j \in \mathcal{U}_t^+(i)$  for  $\mathbf{p}_i \in \mathcal{P}_J$  and  $s_i \approx -\frac{1}{2}$ , i.e.,  $\mathbf{p}_i$  appears in most negative points and almost does not appear in positive points. In this case, as in the previous argument (note that  $s_1 \approx \frac{1}{2}$ ), we should expect that  $\mathbf{u}_t^{(j)} \cdot \mathbf{p}_i$  increases in each iteration and now  $M_{\mathbf{u}}^+(i)$  should be large. Overall, we see that the value  $\frac{-s_i}{s_1}$  approximates well the detection ratio  $\frac{M_{\mathbf{u}}^+(i)}{M_{\mathbf{w}}^+(1)}$  (here we use the assumption that  $|\mathcal{U}_t^+(i)| \approx |\mathcal{W}_t^+(1)|$ ).

On the other hand, if  $\mathbf{p}_i$  appears in roughly an equal number of positive and negative points, i.e.,  $s_i \approx 0$ , then we should expect  $M_{\mathbf{u}}^+(i)$  to be low. To see this, consider a filter  $j \in \mathcal{U}_t^+(i)$ . In this case, positive points that contain  $\mathbf{p}_i$  and with non-zero loss add  $-\frac{\eta}{m} \mathbf{p}_i$  to  $\mathbf{u}_t^{(j)}$ , while negative points that contain  $\mathbf{p}_i$  and have non-zero loss add  $\frac{\eta}{m} \mathbf{p}_i$ . Thus,  $\mathbf{u}_t^{(j)} \cdot \mathbf{p}_i$  should not increase significantly. Therefore, both  $\frac{M_{\mathbf{u}}^+(i)}{M_{\mathbf{w}}^+(1)}$  and  $\frac{-s_i}{s_1}$  should be small in this case.

Given the intuitions above, one possible conjecture is that the detection ratio  $\frac{M_{\mathbf{u}}^+(i)}{M_{\mathbf{w}}^+(1)}$  is bounded by an affine function of  $\max\left(-\frac{s_i}{s_1}, 0\right)$ , which leads to the PSI condition in Definition 4.1.<sup>4</sup> The bias term in the affine function takes into account that our intuition above is not exact. It is reasonable to assume that the bias in the affine function decreases with  $m$ , because the gradient updates are scaled by  $\frac{1}{m}$ . Therefore, any additive error in the weights trajectory is scaled by  $\frac{1}{m}$ . Finally, we can make a similar argument that  $-\frac{s_i}{s_2}$  predicts the value of  $\frac{M_{\mathbf{u}}^-(i)}{M_{\mathbf{u}}^-(2)}$  which appear in the second inequality in Definition 4.1.

## 5. VC Dimension Bounds and Relation to PSI

In Section 3 we defined a classification problem and a neural architecture. In this section we show that this neural architecture is highly expressive, and can thus potentially overfit and generalize poorly. However, as we show later in Sec. 6, if one restricts the class to models with the PSI property, overfitting is avoided.

In Section 5.1, we prove upper and lower bounds on the VC dimension. One particularly interesting consequence of the lower bound proof, is that the networks constructed there for shattering a set do not satisfy the PSI condition. We show this in Sec. 5.2.

<sup>4</sup>We consider  $\max\left(-\frac{s_i}{s_1}, 0\right)$  in the PSI definition because the detection ratios are non-negative.

### 5.1. VC Bounds

First, we give a simple upper bound on the VC dimension. Without considering the order of the patterns in the images, there are at most  $\binom{d}{n}$  input points in  $\mathcal{D}$ . Since the network in Eq. 1 is invariant to the order of the patterns in an image, this implies:

**Proposition 5.1.**  $VC(\mathcal{H}) \leq \binom{d}{n}$ .

Standard VC bounds thus imply that sample complexity for learning in  $\mathcal{H}$  is upper bounded by  $O(\binom{d}{n})$ . Note that this is true regardless of the number of channels  $2k$ .

The lower bound below is more challenging, and reveals interesting connections to the PSI property.

**Theorem 5.2.** *Assume that  $d = 2n$  and  $n \geq 2$ , then  $VC(\mathcal{H}) \geq 2^{\frac{d}{2}-1}$ .*

*Proof.* We will construct a set  $B$  of size  $2^{n-1} = 2^{\frac{d}{2}-1}$  that can be shattered. For a given  $I \in \{0, 1\}^{n-1}$  let  $I[j]$  be its  $j$ th entry. For any such  $I$ , define a point  $\mathbf{x}_I$  such that for any  $1 \leq j \leq n-1$ ,

$$\mathbf{x}_I[j] = I[j] \mathbf{p}_{2j+1} + (1 - I[j]) \mathbf{p}_{2j+2}$$

Furthermore, arbitrarily choose  $\mathbf{x}_I[n] = \mathbf{p}_1$  or  $\mathbf{x}_I[n] = \mathbf{p}_2$ . Define  $B = \{\mathbf{x}_I \mid I \in \{0, 1\}^{n-1}\}$ . Note that  $B$  is a valid set of  $x$  points according to our distribution definition in Section 3.

Now, assume that each point  $\mathbf{x}_I \in B$  has label  $y_I$ . We will show that there is a network  $N \in \mathcal{H}$  such that  $N(\mathbf{x}_I) = y_I$  for all  $I$ . For each  $I \in \{0, 1\}^{n-1}$ , define:

$$\mathbf{w}^{(I)} = \max\{\alpha_I, 0\} \sum_{1 \leq j \leq n-1} \mathbf{x}_I[j] \quad (10)$$

and  $\mathbf{u}^{(I)} = \max\{-\alpha_I, 0\} \sum_{1 \leq j \leq n-1} \mathbf{x}_I[j]$ , where  $\{\alpha_I\}$  is the unique solution of the following linear system with  $2^{n-1}$  equations. For each  $I \in \{0, 1\}^{n-1}$  the system has the following equation:

$$\sum_{I' \in \{0, 1\}^{n-1} \setminus \{I\}} \alpha_{I'} = y_{I^c} \quad (11)$$

where for any  $I \in \{0, 1\}^{n-1}$ ,  $I^c \in \{0, 1\}^{n-1}$  is defined such that  $I^c[j] = 1 - I[j]$  for all  $1 \leq j \leq n-1$ . There is a unique solution because the corresponding matrix of the linear system is the difference between an all 1's matrix and the identity matrix. By the Sherman-Morrison formula (Sherman & Morrison, 1950), this matrix is invertible.

Now, recall that the network output  $N(\mathbf{x})$  is (see Eq. 1)

$$\begin{aligned} & \sum_{I' \in \{0, 1\}^{n-1}} \left[ \max_j \left\{ \sigma(\mathbf{w}^{(I')} \cdot \mathbf{x}[j]) \right\} \right. \\ & \quad \left. - \max_j \left\{ \sigma(\mathbf{u}^{(I')} \cdot \mathbf{x}[j]) \right\} \right] \end{aligned}$$

Then, for any  $\mathbf{x}_I$  we have that:

$$\begin{aligned} N(\mathbf{x}_I) &= \sum_{I' \in \{0,1\}^{n-1}} \alpha_{I'} \max_j \left\{ \sigma \left( \sum_{1 \leq i \leq n-1} \mathbf{x}_{I'}[i] \cdot \mathbf{x}_I[j] \right) \right\} \\ &= \sum_{I' \in \{0,1\}^{n-1}} \alpha_{I'} \max_j \{ \mathbf{x}_{I'}[j] \cdot \mathbf{x}_I[j] \} \\ &= \sum_{I' \in \{0,1\}^{n-1} \setminus \{I^c\}} \alpha_{I'} = y_I \end{aligned}$$

by the definition of  $N$ , the orthogonality of the patterns, and Eq. 11. We have shown that any labeling  $y_I$  can be achieved, and hence the set is shattered, completing the proof.  $\square$

## 5.2. Relation to PSI

The proof of Theorem 5.2 shows that there are exponentially large training sets that can be exactly fit with  $\mathcal{H}$ . This fact can be used to show a lower bound on sample complexity that is exponential in  $d$  for general ERM algorithms (Anthony & Bartlett, 2009). The networks that fit these datasets are those defined by  $\mathbf{w}^{(I)}, \mathbf{u}^{(I)}$ . It is easy to see that these networks *do not* satisfy the PSI property. To see this, note that  $M_{\mathbf{w}}^+(1) = M_{\mathbf{u}}^-(2) = 0$ , which implies that the left-hand sides of parts 1 and 2 in the Definition 4.1 are infinite. Therefore, PSI is not satisfied for these networks.

The networks in Theorem 5.2 classify points based on the patterns  $\mathcal{P}_J$ , and not on the patterns which determine the class. Networks that satisfy PSI are essentially the opposite. Namely, they classify a point mostly based on detectors for the patterns  $\mathbf{p}_1$  and  $\mathbf{p}_2$  and thus generalize well, as we show in the next section.

## 6. PSI Implies Good Generalization

In the previous section we showed that a general ERM algorithm for the class  $\mathcal{H}$  may need exponentially many training samples to get low test error. Here we show that any algorithm satisfying the PSI condition (see Definition 4.1) will have polynomial sample complexity, when patterns in  $\mathcal{P}_J$  are unbiased (i.e.,  $\mathbb{E}[y \mathbb{1}\{\mathbf{p}_i \in \mathbf{x}\}] = 0$  for  $\mathbf{p}_i \in \mathcal{P}_J$ ). Specifically, we show that such an algorithm will have zero *test* error w.h.p., given only  $O(d^2 \log(d))$  training samples. The proof shows that by the assumption  $\mathbb{E}[y \mathbb{1}\{\mathbf{p}_i \in \mathbf{x}\}] = 0$ ,  $s_i$  should be small and therefore the detection ratios should be small by PSI. Then, by the key observation on detection ratios (Eq. 5 and Eq. 8), the algorithms obtains zero test error. We summarize the result in the following theorem.

**Theorem 6.1.** *Assume that  $\mathcal{D}$  satisfies the conditions in Section 3 and  $\mathbb{E}[y \mathbb{1}\{\mathbf{p}_i \in \mathbf{x}\}] = 0$  for all  $\mathbf{p}_i \in \mathcal{P}_J$ . Let  $\mathcal{A}$  be a learning algorithm which satisfies  $(b, c, \delta)$ -PSI with  $b, c \geq 1$ . Then, if  $m > 300b^2c^2d^2 \log(d)$ , with probability at least  $1 - \delta - \frac{4}{d^3}$ ,<sup>5</sup>  $\mathcal{A}(\mathcal{S})$  has 0 test error with respect to  $\mathcal{D}$ .*

<sup>5</sup>We note that the  $\frac{4}{d^3}$  may be improved to an arbitrary  $\gamma > 0$  if

*Proof.* By the assumption, for  $\mathbf{p}_i \in \mathcal{P}_J$ ,  $s_i$  is an average of  $m$  IID binary variables  $y_j \mathbb{1}\{\mathbf{p}_i \in \mathbf{x}_j\}$  with zero expected value. Thus, by Hoeffding's inequality we have for all  $\mathbf{p}_i \in \mathcal{P}_J$  that:

$$\mathbb{P} \left( b|s_i| \leq 4b \sqrt{\frac{\log(d)}{m}} \right) \leq \frac{2}{d^4}$$

Therefore, by a union bound over all patterns  $\mathbf{p}_i \in \mathcal{P}_J$  (recall  $|\mathcal{P}| \leq d$ ), with probability at least  $1 - \frac{2}{d^3}$ , for all  $\mathbf{p}_i \in \mathcal{P}_J$ :

$$b|s_i| \leq 4b \sqrt{\frac{\log(d)}{m}} \leq \frac{1}{6cd} \quad (12)$$

Next we consider  $\mathbf{p}_1$  (the positive pattern), for which  $\mathbb{E}[s_1] = 0.5$  (because it only appears in the positive examples, and the prior over  $y$  is 0.5). Hoeffding's bound and the definition of  $m$  imply that  $|s_1| \geq \frac{1}{3}$  with probability at least  $1 - \frac{1}{d^3}$ .<sup>6</sup>

We can now do a union bound over all patterns and PSI condition to obtain that with probability at least  $1 - \delta - \frac{3}{d^3}$  we have by the PSI property and Eq. 12, for all  $\mathbf{p}_i \in \mathcal{P}_J$ :

$$\frac{M_{\mathbf{u}}^+(i)}{M_{\mathbf{w}}^+(1)} \leq b \frac{|s_i|}{|s_1|} + \frac{c}{\sqrt{m}} \leq \frac{1}{2cd} + \frac{c}{\sqrt{m}} < \frac{1}{d} \quad (13)$$

Furthermore, by PSI we have  $\frac{M_{\mathbf{u}}^+(1)}{M_{\mathbf{w}}^+(1)} \leq \frac{c}{\sqrt{m}} < \frac{1}{d}$ .

Therefore, for any positive point  $(\mathbf{x}^+, 1)$  we have by Eq. 5:

$$N_W^k(\mathbf{x}^+) > M_{\mathbf{w}}^+(1) \left( 1 - \frac{d-1}{d} \right) > 0$$

Thus,  $\mathbf{x}^+$  is classified correctly. By the symmetry of the problem and part 2 in Definition 4.1, any negative point will be classified correctly as well.  $\square$

## 7. SGD satisfies PSI - Empirical Analysis

Thus far we have established that the PSI property implies good generalization. Here we provide empirical evidence that SGD indeed learns such models with overparameterized CNNs. In Section 7.1, we empirically validate the PSI condition. In Section 7.2, we provide a qualitative analysis that confirms that the statistics of the patterns in the training set correlate with the dot product between a detector and its detected pattern. Details of the experiments are provided in the supplementary.

we scale  $m$  by  $\log \gamma$ .

<sup>6</sup>In fact we can have exponential dependence here, but we use  $d^3$  to simplify later expressions.

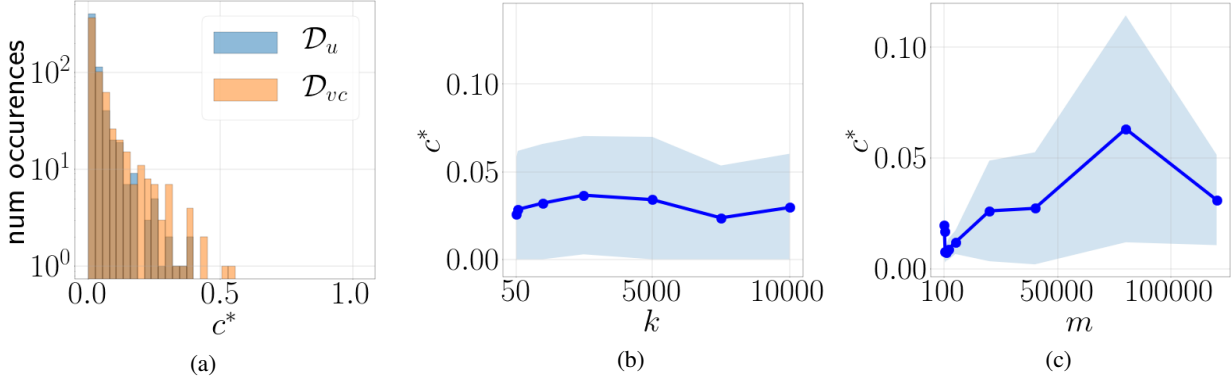


Figure 2. Empirical analysis of  $c^*$ . (a) Empirical calculation of  $c^*$  for  $\mathcal{D}_u$  and  $\mathcal{D}_{vc}$ . Values are in log scale. (b)  $c^*$  as a function of the network size  $k$  (c)  $c^*$  as a function of the training set size  $m$ .

### 7.1. Empirical Validation of PSI

We perform experiments with two types of distributions that satisfy the properties defined in Section 3. They differ in the random sampling procedure of joint patterns described in Section 3.

- Given  $y = 1$  or  $y = -1$ , the distribution denoted by  $\mathcal{D}_u$  selects  $n - 1$  patterns uniformly at random without replacement from  $\mathcal{P}_J$ .
- Assume that  $d = 2n$ . Given  $y = 1$  or  $y = -1$ , for each  $1 \leq j \leq n - 1$  the distribution  $\mathcal{D}_{vc}$  selects one pattern from  $\{\mathbf{p}_{2j+1}, \mathbf{p}_{2j+2}\}$  uniformly at random.

Both  $\mathcal{D}_u$  and  $\mathcal{D}_{vc}$  satisfy  $\mathbb{E}[y \mathbb{1}\{\mathbf{p}_i \in \mathcal{P}\}] = 0$  for all  $\mathbf{p}_i \in \mathcal{P}_J$ . Thus, given Theorem 6.1 if we can show the PSI condition holds, good generalization will be implied.

**Remark 7.1.** *The support of  $\mathcal{D}_{vc}$  is the shattered set  $B$  in the proof of Theorem 5.2. The proof implies that for any sampled training and test sets which are subsets of  $B$ , there exists a network with 0 training error and arbitrarily high test error. Therefore, by optimizing the training error, SGD can converge to these solutions. However, as we show next, SGD does not converge to these solutions, but rather it satisfies PSI and converges to solutions with good generalization performance.*

To empirically validate PSI and show that it implies good generalization, we could in principle show that the conditions of Theorem 6.1 hold empirically, i.e., there exist  $b, c$  and  $m$  such that  $m > 300b^2c^2d^2 \log(d)$  and PSI holds with constants  $b, c$  and high probability  $1 - \delta$ . However, as with most generalization results, the bound is not exact up to constants and using its numerical value results in large  $m$  which cannot be empirically tested.

Instead, we show that for empirically large  $m$ , PSI holds

with small constants  $b$  and  $c$  which do not change the order of magnitude of the bound, namely,  $b^2c^2 < 10$ . Indeed, we will show empirically that  $b^2c^2 \leq 4$  across a large number of experiments.

We trained a neural network in our setting with SGD as described in Section 3. We performed more than 1000 experiments with parameter values  $100 \leq m \leq 40000$ ,  $1000 \leq k \leq 10000$ ,  $(n, d) \in \{(10, 20), (10, 80), (20, 50), (40, 60)\}$  for  $\mathcal{D} = \mathcal{D}_u$  and  $(n, d) \in \{(10, 20), (40, 80), (25, 50), (30, 60)\}$  for  $\mathcal{D} = \mathcal{D}_{vc}$ . For each distribution  $\mathcal{D}_u$  or  $\mathcal{D}_{vc}$ , we performed 10 experiments for each set of values for  $n, d, k$  and  $m$ . For each experiment, we set  $b = 2$  and empirically calculated the lowest constant  $c$  which satisfies the PSI definition, which we denote by  $c^*$ . Formally,

$$c^* = \sqrt{m} \max \left\{ \max_{i \in \mathcal{P}_J \cup \mathcal{P}_+} \Psi_1^{(i)}, \max_{i \in \mathcal{P}_J \cup \mathcal{P}_-} \Psi_2^{(i)}, 0 \right\}$$

where:

$$\begin{aligned} \Psi_1^{(i)} &= \frac{M_{\mathbf{u}}^+(i)}{M_{\mathbf{w}}^+(1)} - 2 \max \left( -\frac{s_i}{s_1}, 0 \right) \\ \Psi_2^{(i)} &= \frac{M_{\mathbf{u}}^-(i)}{M_{\mathbf{w}}^-(2)} - 2 \max \left( -\frac{s_i}{s_2}, 0 \right) \end{aligned}$$

Figure 2a shows that across all experiments the value of  $c^*$  is less than 1.

To further validate the PSI condition, we tested whether the conditions in the proof of Theorem 6.1 empirically hold. Specifically, in the proof we showed that  $\frac{M_{\mathbf{u}}^+(i)}{M_{\mathbf{w}}^+(1)} < \frac{1}{d}$  for all  $\mathbf{p}_i \in \mathcal{P}_J$  (in Eq. 13). We checked this for all settings of  $(n, d)$  and largest possible  $k$  and  $m$ ,  $k = 10000$  and  $m = 40000$ . In all of our experiments, SGD converged to a solution with 0 test error such that Eq. 13 holds for all  $\mathbf{p}_i \in \mathcal{P}_J$ .

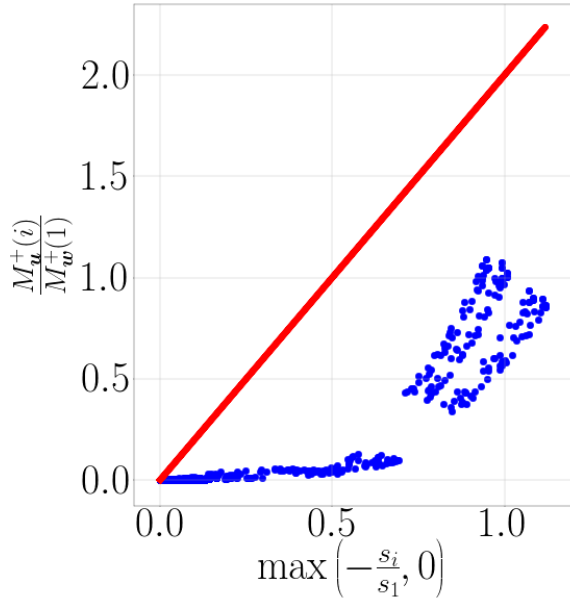


Figure 3. Positive correlation between  $\frac{M_u^+(i)}{M_w^+(1)}$  and  $\max\left(-\frac{s_i}{s_1}, 0\right)$ . The depicted line is the best PSI bound with  $b = 2$  (lowest  $c$ ).

Finally, we checked how  $c^*$  varies with  $k$  and  $m$ . We checked this for  $\mathcal{D} = \mathcal{D}_u$ ,  $d = 50$  and  $n = 20$ . Figure 2b and Figure 2c show that  $c^*$  is at most slightly correlated with  $k$  and  $m$  and has low value for large  $k$  and large  $m$ .

## 7.2. Qualitative Analysis of Inductive Bias

The intuition we described in Section 4, suggests that there is a positive correlation between  $\frac{M_u^+(i)}{M_w^+(1)}$  and  $\max\left(-\frac{s_i}{s_1}, 0\right)$ . To test this, we experimented with a distribution  $\mathcal{D}_p$  which can vary the probability of a joint pattern to be selected and thus can control  $\max\left(-\frac{s_i}{s_1}, 0\right)$ . Given  $y = 1$  it selects  $\mathbf{p}_3$  with probability  $p$  or  $\mathbf{p}_4$  with probability  $1-p$ . Then it selects the remaining  $n-2$  patterns from  $\mathcal{P}_J \setminus \{\mathbf{p}_3, \mathbf{p}_4\}$  uniformly at random without replacement. Similarly, given  $y = -1$  it selects  $\mathbf{p}_3$  with probability  $1-p$  or  $\mathbf{p}_4$  with probability  $p$ . The remaining  $n-2$  patterns are selected uniformly without replacement from  $\mathcal{P}_J \setminus \{\mathbf{p}_3, \mathbf{p}_4\}$ . We experimented with various  $p$  and plotted for each solution of SGD,  $\frac{M_u^+(i)}{M_w^+(1)}$  and  $\max\left(-\frac{s_i}{s_1}, 0\right)$  for all  $\mathbf{p}_i \in \mathcal{P}_J \cup \mathcal{P}_+$ . Figure 3 clearly shows a positive correlation between these quantities, strongly suggesting that SGD results in large dot products between the detectors and detected patterns that are biased towards a certain class.

## 8. SGD satisfies PSI - Optimization Analysis

In this section we show that PSI holds for a simple setup of two points in the training set. We assume that the training set consists of two points and denote  $S = \{(\mathbf{x}^+, 1), (\mathbf{x}^-, -1)\}$ . We further assume that  $\mathbf{x}^+$  and  $\mathbf{x}^-$  have exactly the same patterns in  $\mathcal{P}_J$ . Note that in this case we have  $s_1 = -s_2 = 1$  and  $s_i = 0$  for all  $\mathbf{p}_i \in \mathcal{P}_J$ . We analyze gradient descent and assume that it runs with a constant learning rate  $\eta = \frac{c_\eta}{k}$ . We denote  $a \ll b$  if  $a > 0$  is sufficiently small compared to  $b > 0$ , e.g.,  $a \leq \frac{b}{100}$ .

The following theorem shows that PSI holds with constants  $b = 1$  and  $c = \sqrt{18c_\eta}$ . The proof analyzes the trajectory of gradient descent and is provided in the supplementary.

**Theorem 8.1.** *For a sufficiently small  $\epsilon$ ,  $\sigma_g$ ,  $c_\eta$  such that  $\sigma_g \ll \eta$  and  $k \geq \text{poly}(\log d, \frac{1}{\epsilon})$ , with probability at least  $1 - \frac{9}{d^7} - 8e^{-8}$ , gradient descent converges to a global minimum with parameters  $W$  after  $T \leq O\left(\frac{1}{c_\eta}\right)$  iterations and the following holds:*

1. For all  $\mathbf{p}_i \in \mathcal{P}_J \cup \mathcal{P}_+$ , we have:

$$\frac{M_u^+(i)}{M_w^+(1)} \leq \max\left(-\frac{s_i}{s_1}, 0\right) + 3c_\eta$$

2. For all  $\mathbf{p}_i \in \mathcal{P}_J \cup \mathcal{P}_-$ :

$$\frac{M_w^-(i)}{M_u^-(2)} \leq \max\left(-\frac{s_i}{s_2}, 0\right) + 3c_\eta$$

Therefore, the PSI condition is satisfied with  $b = 1$  and  $c = \sqrt{18c_\eta}$ .

Notice that the theorem holds for overparameterized networks (sufficiently large  $k$ ), which coincides with our empirical findings in the previous section. Finally, we note that the theorem holds for sufficiently small initialization, and thus it is not in the same regime of NTK analysis where initialization is relatively large (Woodworth et al., 2019; Chizat et al., 2019).

## 9. Conclusions

Understanding the inductive bias of gradient methods for deep learning is an important challenge. In this paper, we identify a new form of inductive bias for CNNs and provide theoretical and empirical support that SGD exhibits this bias and consequently has good generalization performance.

We use a unique approach of combining novel empirical observations with theoretical guarantees to make headway in a challenging setting of non-linear overparameterized CNNs. We believe that this can pave the way for studying inductive bias in other difficult settings. Extending the PSI notion to other neural architectures and distributions is an interesting direction for future work.

## Acknowledgements

This research is supported by the Blavatnik Computer Science Research Fund and by the European Research Council (ERC) under the European Unions Horizon 2020 research and innovation programme (grant ERC Holi 819080). We thank Roi Livni for helpful discussions.

## References

Anthony, M. and Bartlett, P. L. *Neural network learning: Theoretical foundations*. cambridge university press, 2009.

Arora, S., Cohen, N., Hu, W., and Luo, Y. Implicit regularization in deep matrix factorization. In *Advances in Neural Information Processing Systems*, pp. 7411–7422, 2019a.

Arora, S., Du, S., Hu, W., Li, Z., and Wang, R. Fine-grained analysis of optimization and generalization for overparameterized two-layer neural networks. In *International Conference on Machine Learning*, pp. 322–332, 2019b.

Bai, Y. and Lee, J. D. Beyond linearization: On quadratic and higher-order approximation of wide neural networks. *arXiv preprint arXiv:1910.01619*, 2019.

Brutzkus, A. and Globerson, A. Globally optimal gradient descent for a convnet with gaussian inputs. In *International Conference on Machine Learning*, pp. 605–614, 2017.

Brutzkus, A. and Globerson, A. Why do larger models generalize better? a theoretical perspective via the xor problem. In *International Conference on Machine Learning*, pp. 822–830, 2019.

Brutzkus, A., Globerson, A., Malach, E., and Shalev-Shwartz, S. Sgd learns over-parameterized networks that provably generalize on linearly separable data. *International Conference on Learning Representations*, 2018.

Chizat, L., Oyallon, E., and Bach, F. On lazy training in differentiable programming. In *Advances in Neural Information Processing Systems*, pp. 2933–2943, 2019.

Du, S., Lee, J., Tian, Y., Singh, A., and Poczos, B. Gradient descent learns one-hidden-layer cnn: Dont be afraid of spurious local minima. In *International Conference on Machine Learning*, pp. 1339–1348, 2018a.

Du, S., Lee, J., Li, H., Wang, L., and Zhai, X. Gradient descent finds global minima of deep neural networks. In *International Conference on Machine Learning*, pp. 1675–1685, 2019.

Du, S. S., Lee, J. D., and Tian, Y. When is a convolutional filter easy to learn? *ICLR*, 2018b.

Du, S. S., Zhai, X., Poczos, B., and Singh, A. Gradient descent provably optimizes over-parameterized neural networks. *International Conference on Learning Representations*, 2018c.

Fiat, J., Malach, E., and Shalev-Shwartz, S. Decoupling gating from linearity. *arXiv preprint arXiv:1906.05032*, 2019.

Ji, Z. and Telgarsky, M. Risk and parameter convergence of logistic regression. *arXiv preprint arXiv:1803.07300*, 2018.

Ji, Z. and Telgarsky, M. Gradient descent aligns the layers of deep linear networks. *ICLR*, 2019.

Krizhevsky, A., Sutskever, I., and Hinton, G. E. Imagenet classification with deep convolutional neural networks. In *Advances in neural information processing systems*, pp. 1097–1105, 2012.

Lyu, K. and Li, J. Gradient descent maximizes the margin of homogeneous neural networks. *arXiv preprint arXiv:1906.05890*, 2019.

Nacson, M. S., Gunasekar, S., Lee, J., Srebro, N., and Soudry, D. Lexicographic and depth-sensitive margins in homogeneous and non-homogeneous deep models. In *International Conference on Machine Learning*, pp. 4683–4692, 2019.

Sherman, J. and Morrison, W. J. Adjustment of an inverse matrix corresponding to a change in one element of a given matrix. *The Annals of Mathematical Statistics*, 21(1):124–127, 1950.

Soudry, D., Hoffer, E., Nacson, M. S., Gunasekar, S., and Srebro, N. The implicit bias of gradient descent on separable data. *The Journal of Machine Learning Research*, 19(1):2822–2878, 2018.

Taigman, Y., Yang, M., Ranzato, M., and Wolf, L. Deepface: Closing the gap to human-level performance in face verification. In *Proceedings of the IEEE conference on computer vision and pattern recognition*, pp. 1701–1708, 2014.

Wei, C., Lee, J. D., Liu, Q., and Ma, T. Regularization matters: Generalization and optimization of neural nets vs their induced kernel. In *Advances in Neural Information Processing Systems*, pp. 9709–9721, 2019.

Woodworth, B., Gunasekar, S., Lee, J., Soudry, D., and Srebro, N. Kernel and deep regimes in overparametrized models. *arXiv preprint arXiv:1906.05827*, 2019.

Xu, K., Ba, J., Kiros, R., Cho, K., Courville, A., Salakhudinov, R., Zemel, R., and Bengio, Y. Show, attend and

tell: Neural image caption generation with visual attention. In *International conference on machine learning*, pp. 2048–2057, 2015.

Yehudai, G. and Shamir, O. On the power and limitations of random features for understanding neural networks. In *Advances in Neural Information Processing Systems*, pp. 6594–6604, 2019.

Yu, B., Zhang, J., and Zhu, Z. On the learning dynamics of two-layer nonlinear convolutional neural networks. *arXiv preprint arXiv:1905.10157*, 2019.

Zhang, C., Bengio, S., Hardt, M., Recht, B., and Vinyals, O. Understanding deep learning requires rethinking generalization. *ICLR*, 2017.

---

## Supplementary material

---

### A. Experimental Details in Section 7

Here we provide details of the experiments performed in Section 7. All experiments were run on NVidia Titan Xp GPUs with 12GB of memory. Training algorithms were implemented in TensorFlow. All of the empirical results can be replicated in approximately 150 hours on a single Nvidia Titan Xp GPU.

#### A.1. Figure 2a Experiment

We performed more than 1000 experiments with the network in Eq. 1 and SGD. We experimented with parameter values  $k \in \{1000, 10000\}$ ,  $m \in \{100, 500, 1000, 2000, 5000, 20000, 40000\}$ ,  $(n, d) \in \{(10, 20), (10, 80), (20, 50), (40, 60)\}$  for  $\mathcal{D} = \mathcal{D}_u$  and  $(n, d) \in \{(10, 20), (40, 80), (25, 50), (30, 60)\}$  for  $\mathcal{D} = \mathcal{D}_{vc}$ . For each distribution  $\mathcal{D}_u$  or  $\mathcal{D}_{vc}$ , we performed 10 experiments for each set of values for  $n$ ,  $d$ ,  $k$  and  $m$ . For each set of values we plot the mean of the 10 experiments and standard deviation error bars in shaded regions. In each one of the 10 experiments we randomly sampled the training and test sets according to the given distribution  $\mathcal{D}_u$  or  $\mathcal{D}_{vc}$  and randomly sampled the initialization of the network. We used a test set of size 1000. All orthogonal patterns were one-hot vectors. We trained only the weights of the first convolutional layer. We used a batch size of 20 if  $k = 10000$  and batch size of 100 for  $k = 1000$ . The learning rate was set to  $\max\{\frac{0.001}{2k}, 0.000001\}$  and  $\sigma_g$  to 0.000001. The solution SGD returned was either after 50000 epochs or if there was an epoch where the training loss was less than 0.00001. For each experiment, we set  $b = 2$  and empirically calculated  $c^*$ .

#### A.2. Figure 2b Experiment

In the same setup of Section A.1 (i.e., batch size, stopping criteria, learning rate etc.), we performed experiments with distribution  $\mathcal{D}_u$ ,  $n = 20$ ,  $d = 50$ ,  $m = 2000$  and  $k \in \{50, 100, 1000, 2500, 5000, 7500, 10000\}$ .

#### A.3. Figure 2c Experiment

In the same setup of Section A.1, we performed experiments with distribution  $\mathcal{D}_u$ ,  $n = 20$ ,  $d = 50$ ,  $k = 2500$  and  $m \in \{100, 200, 500, 1000, 2000, 5000, 20000, 40000, 80000, 120000\}$ .

#### A.4. Figure 3 Experiment

In the setup of Section A.1 we experimented with distributions  $\mathcal{D}_p$  for  $p$  values in

$$\{0.0, 0.01, 0.03, 0.05, 0.07, 0.1, 0.12, 0.2, 0.21, 0.28, 0.3, 0.4, 0.44, 0.5, 0.51, 0.59, 0.6, 0.68, 0.7, 0.78, 0.8, 0.9, 0.91, 0.94, 0.95, 0.98, 0.99, 1.0\}$$

We experimented with values  $n = 40$ ,  $d = 60$ ,  $m = 1000$  and  $k = 2500$ . The solution SGD returned was either after 2000 epochs or if there was an epoch where the training loss was less than 0.00001.

## B. Proof of Theorem 8.1

### B.1. Notations

Here we define additional notations that will be useful for the proof of the theorem.

Let  $\mathcal{P}_S$  be the set of all patterns that appear in either  $x^+$  or  $x^-$ . Define:

$$\begin{aligned}\mathcal{W}_t^+(i) &= \left\{ j \mid \arg \max_{l \in \mathcal{P}_S \setminus \{2\}} \mathbf{w}_t^{(j)} \cdot \mathbf{p}_l = i, \mathbf{w}_t^{(j)} \cdot \mathbf{p}_i > 0 \right\} \\ \mathcal{U}_t^+(i) &= \left\{ j \mid \arg \max_{l \in \mathcal{P}_S \setminus \{2\}} \mathbf{u}_t^{(j)} \cdot \mathbf{p}_l = i, \mathbf{u}_t^{(j)} \cdot \mathbf{p}_i > 0 \right\}\end{aligned}\quad (14)$$

and

$$\begin{aligned}\mathcal{W}_t^-(i) &= \left\{ j \mid \arg \max_{l \in \mathcal{P}_S \setminus \{1\}} \mathbf{w}_t^{(j)} \cdot \mathbf{p}_l = i, \mathbf{w}_t^{(j)} \cdot \mathbf{p}_i > 0 \right\} \\ \mathcal{U}_t^-(i) &= \left\{ j \mid \arg \max_{l \in \mathcal{P}_S \setminus \{1\}} \mathbf{u}_t^{(j)} \cdot \mathbf{p}_l = i, \mathbf{u}_t^{(j)} \cdot \mathbf{p}_i > 0 \right\}\end{aligned}\quad (15)$$

Define:

$$\begin{aligned}A_{\mathbf{w}} &= \bigcup_{i \in \mathcal{P}_S \setminus \{2\}} \mathcal{W}_0^+(i) \\ A_{\mathbf{u}} &= \bigcup_{i \in \mathcal{P}_S \setminus \{1\}} \mathcal{U}_0^-(i)\end{aligned}$$

Finally we define  $\text{poly}(x)$  to be any polynomial function of  $x$ .

## B.2. Auxiliary Lemmas

We now prove several technical lemmas. In Section B.3 we use the lemmas to prove the theorem. In the next 3 lemmas we provide high probability bounds on sizes of certain sets that are functions of the sets in Eq. 14 and Eq. 15.

**Lemma B.1.** *For any  $0 < \epsilon < \frac{1}{4}$ , with probability at least  $1 - 4e^{-8}$  for any  $k > \text{poly}(\frac{1}{\epsilon})$ :*

$$\left| \frac{|A_{\mathbf{w}}|}{k} - (1 - 2^{-n}) \right| \leq \epsilon$$

and

$$\left| \frac{|A_{\mathbf{u}}|}{k} - (1 - 2^{-n}) \right| \leq \epsilon$$

*Proof.* It suffices to show that for any  $k$ :

$$|A_{\mathbf{w}}| - (1 - 2^{-n}) k \leq 2\sqrt{k}$$

and

$$|A_{\mathbf{u}}| - (1 - 2^{-n}) k \leq 2\sqrt{k}$$

For each  $1 \leq j \leq k$  it holds that  $j \in A_{\mathbf{w}}$  with probability  $1 - 2^{-n}$ . Therefore by Hoeffding's inequality, with probability at least  $1 - 2e^{-8}$ ,

$$|A_{\mathbf{w}}| - (1 - 2^{-n}) k \leq 2\sqrt{k}.$$

The same argument applies for  $|A_{\mathbf{u}}|$ , a union bound and setting  $k > \frac{1}{\epsilon^3}$  concludes the proof.  $\square$

**Lemma B.2.** *For any  $\epsilon > 0$ , with probability at least  $1 - \frac{4}{d^7} - 4e^{-8}$ , for  $k > \text{poly}(\log d, \frac{1}{\epsilon})$  and for all  $i \in \mathcal{P}_S \setminus \{2\}$ :*

$$\frac{|\mathcal{W}_0^+(i)|}{k(1 - 2^{-n} + \epsilon)} \leq \frac{1}{n} + \epsilon$$

and

$$\frac{|\mathcal{W}_0^+(i)|}{k(1-2^{-n}-\epsilon)} \geq \frac{1}{n} - \epsilon$$

Similarly, for all  $i \in \mathcal{P}_S \setminus \{1\}$  :

$$\frac{|\mathcal{U}_0^-(i)|}{k(1-2^{-n}+\epsilon)} \leq \frac{1}{n} + \epsilon$$

and

$$\frac{|\mathcal{U}_0^-(i)|}{k(1-2^{-n}-\epsilon)} \geq \frac{1}{n} - \epsilon$$

*Proof.* Without loss of generality, consider  $|\mathcal{W}_0^+(i)|$ . We first condition on the random variable  $|A_w|$  and given that the event  $k(1-2^{-n}-\epsilon) \leq |A_w| \leq k(1-2^{-n}+\epsilon)$  holds. By symmetry, we have  $\mathbb{E} \left[ \frac{|\mathcal{W}_0^+(i)|}{|A_w|} \right] = \frac{1}{n}$  where the expectation is with respect to the initialization. Thus, we get by Hoeffding's inequality:

$$\begin{aligned} \mathbb{P} \left( \left| \frac{|\mathcal{W}_0^+(i)|}{|A_w|} - \frac{1}{n} \right| \leq \frac{2\sqrt{\log d}}{\sqrt{|A_w|}} \right) \\ \leq 2e^{-2|A_w| \left( \frac{2\sqrt{\log d}}{\sqrt{|A_w|}} \right)^2} = \frac{2}{d^8} \end{aligned}$$

By the law of total probability, applying Lemma B.1 and a union bound over  $i \in \mathcal{P}_S$  twice (for both  $\mathcal{W}_0^+(i)$  and  $\mathcal{U}_0^-(i)$ ), we get the desired result.  $\square$

**Lemma B.3.** For any  $\epsilon > 0$ , with probability at least  $1 - \frac{4}{d^7} - 4e^{-8}$ , for  $k > \text{poly}(\log d, \frac{1}{\epsilon})$  and for all  $i \in \mathcal{P}_S \setminus \{1, 2\}$  the following holds:

$$\begin{aligned} \frac{|\mathcal{W}_0^+(i) \cap \mathcal{W}_0^-(2)|}{k(\frac{1}{2} - 2^{-n-1} + \epsilon)} &\leq \frac{1}{n(n+1)} + \epsilon \\ \frac{|\mathcal{W}_0^+(i) \cap \mathcal{W}_0^-(2)|}{k(\frac{1}{2} - 2^{-n-1} - \epsilon)} &\geq \frac{1}{n(n+1)} - \epsilon \\ \frac{|\mathcal{U}_0^+(1) \cap \mathcal{U}_0^-(i)|}{k(\frac{1}{2} - 2^{-n-1} + \epsilon)} &\leq \frac{1}{n(n+1)} + \epsilon \end{aligned}$$

and

$$\frac{|\mathcal{U}_0^+(1) \cap \mathcal{U}_0^-(i)|}{k(\frac{1}{2} - 2^{-n-1} - \epsilon)} \geq \frac{1}{n(n+1)} - \epsilon$$

*Proof.* The proof is similar to the proofs of Lemma B.1 and Lemma B.2. The difference is that we use the equalities  $\mathbb{E}[|A_w \cap \mathcal{W}_0^-(2)|] = \mathbb{E}[|A_u \cap \mathcal{U}_0^+(1)|] = (\frac{1}{2} - 2^{-n-1})k$  instead of  $\mathbb{E}[|A_w|] = \mathbb{E}[|A_u|] = (1 - 2^{-n})k$  as in Lemma B.1. Furthermore, we use  $\mathbb{E} \left[ \frac{|\mathcal{W}_0^+(i) \cap \mathcal{W}_0^-(2)|}{|A_w \cap \mathcal{W}_0^-(2)|} \right] = \mathbb{E} \left[ \frac{|\mathcal{U}_0^+(1) \cap \mathcal{U}_0^-(i)|}{|A_u \cap \mathcal{U}_0^+(1)|} \right] = \frac{1}{n(n+1)}$  for fixed  $|A_w \cap \mathcal{W}_0^-(2)|$  and  $|A_u \cap \mathcal{U}_0^+(1)|$  instead of  $\mathbb{E} \left[ \frac{|\mathcal{W}_0^+(i)|}{|A_w|} \right] = \mathbb{E} \left[ \frac{|\mathcal{U}_0^-(i)|}{|A_u|} \right] = \frac{1}{n}$  for fixed  $|A_w|$  and  $|A_u|$  as in Lemma B.2.  $\square$

**Lemma B.4.** For any  $M > 0$  and  $\delta > 0$ , there exists a sufficiently small  $\sigma_g > 0$ , such that with probability at least  $1 - \delta$ , for all  $1 \leq i \leq k$ ,  $\|\mathbf{w}_0^{(i)}\| \leq M$  and  $\|\mathbf{u}_0^{(i)}\| \leq M$ .

*Proof.* The proof is immediate.  $\square$

We now proceed to analyze the dynamics of gradient descent in the next two lemmas. Define  $M$  such that for all  $1 \leq i \leq k$ ,  $\|\mathbf{w}_0^{(i)}\| \leq M$  and  $\|\mathbf{u}_0^{(i)}\| \leq M$ . Let  $\mathcal{E}$  be the set of all  $t$  such that for all  $\mathbf{x} \in S$ , it holds that  $N_{W_t}(\mathbf{x}) < 1$ . Let  $t^* = \arg \min_t \{t - 1 \in \mathcal{E}, t \notin \mathcal{E}\}$ . We assume that  $\eta$  and  $\sigma_g$  are sufficiently small such that  $t^* \geq 2$ .

**Lemma B.5.** For a sufficiently small  $\epsilon, M, c_\eta$  such that  $M \ll \eta$ , the following holds for any  $1 \leq t \leq t^*$ :

1. If  $j \notin A_w$ , then  $w_t^{(j)} = w_0^{(j)} - \alpha \frac{\eta}{2} p_2$  where  $\alpha \in \{0, 1\}$ .
2. If  $j \in \mathcal{W}_0^+(1)$ , then  $w_t^{(j)} = w_0^{(j)} - \frac{\eta}{2} \sum_{i \in \mathcal{P}_S \setminus \{1\}} \alpha_i p_i + \frac{\eta t}{2} p_1$ , where  $\alpha_i \in \{0, 1\}$ .
3. If  $i \in \mathcal{P}_S \cap \mathcal{P}_J$  and  $j \in \mathcal{W}_0^+(i) \cap \mathcal{W}_0^-(i)$  then  $w_t^{(j)} = w_0^{(j)}$ .
4. If  $i \in \mathcal{P}_S \cap \mathcal{P}_J$  and  $j \in \mathcal{W}_0^+(i) \cap \mathcal{W}_0^-(2)$ , then  $w_t^{(j)} = w_0^{(j)} - \frac{\eta}{2} p_2 + \frac{\eta}{2} p_i$
5. If  $j \notin A_u$ , then  $u_t^{(j)} = u_0^{(j)} - \alpha p_1$  where  $\alpha \in \{0, 1\}$ .
6. If  $j \in \mathcal{U}_0^-(2)$ , then  $u_t^{(j)} = u_0^{(j)} - \frac{\eta}{2} \sum_{i \in \mathcal{P}_S \setminus \{2\}} \alpha_i p_i + \frac{\eta t}{2} p_2$ , where  $\alpha_i \in \{0, 1\}$ .
7. If  $i \in \mathcal{P}_S \cap \mathcal{P}_J$  and  $j \in \mathcal{U}_0^-(i) \cap \mathcal{U}_0^+(1)$  then  $u_t^{(j)} = u_0^{(j)}$ .
8. If  $i \in \mathcal{P}_S \cap \mathcal{P}_J$  and  $j \in \mathcal{U}_0^-(i) \cap \mathcal{U}_0^+(1)$ , then  $u_t^{(j)} = u_0^{(j)} - \frac{\eta}{2} p_1 + \frac{\eta}{2} p_i$

*Proof.* 1. If  $j \notin \mathcal{W}_0^-(2)$ , then for  $t = 1$  the gradient of the loss with respect to  $w^{(i)}$  is 0, because every pattern in  $\mathcal{P}_S$  has a negative dot product with  $w_0^{(i)}$ . Therefore,  $w_1^{(i)} = w_0^{(i)}$ . By the same argument  $w_t^{(i)} = w_0^{(i)}$  for all  $t \geq 1$ . If  $j \in \mathcal{W}_0^-(2)$  then  $\frac{\eta}{2} p_2$  will be subtracted in the first iteration, and  $w_t^{(i)}$  will not change in later iterations.

2. The proof follows directly by the gradient update. In each iteration,  $\frac{\eta}{2} p_1$  is added and a pattern in  $\mathcal{P}_S \setminus \{1\}$  is subtracted unless all such patterns already have a negative dot product with  $w_t^{(i)}$ . Note that we used here the fact that  $M \ll \eta$ .
3. For  $t = 1$  we have by the gradient update:

$$w_1^{(j)} = w_0^{(j)} + \frac{\eta}{2} p_1 - \frac{\eta}{2} p_i = w_0^{(j)} \quad (16)$$

By induction,  $w_t^{(i)} = w_0^{(i)}$  for all  $1 \leq t \leq t^*$ .

4. The proof follows by the gradient update as in previous proofs. For  $t = 1$ , the term  $\frac{\eta}{2} p_2$  is subtracted by the update of  $x^-$ , since  $j \in \mathcal{W}_0^-(2)$ . The term  $\frac{\eta}{2} p_i$  is added due to the update of  $x^+$ . Now  $j \in \mathcal{W}_1^+(i) \cap \mathcal{W}_1^-(i)$  and thus  $w_t^{(j)}$  will not change in subsequent iterations, as in the proof of part 3. This concludes the proof.

By symmetry, the proofs of 5-8 are identical to the proofs of parts 1-4.  $\square$

Define

$$\gamma = \frac{(1 - 2^{-n})}{n} \quad (17)$$

then we have the following:

**Lemma B.6.** For a sufficiently small  $\epsilon$ ,  $M$ ,  $c_\eta$  such that  $M \ll \eta$  and  $k \geq \text{poly}(\log d, \frac{1}{\epsilon})$  with probability at least  $1 - \frac{9}{d^7} - 8e^{-8}$ , gradient descent converges to a global minimum after  $\frac{1}{\gamma c_\eta} \leq T \leq \frac{3}{\gamma c_\eta}$  iterations.

*Proof.* Throughout the proof we use Lemma B.4 to choose a sufficiently small  $M$  such that  $|w_0^{(i)}| \leq M$  and  $|u_0^{(i)}| \leq M$  with probability at least  $1 - \frac{1}{d^7}$ . We further apply Lemma B.1, Lemma B.2 and Lemma B.3 which together with Lemma B.4 hold with probability at least  $1 - \frac{9}{d^7} - 8e^{-8}$ . Define the sets of weights  $B_i$  such that  $i$  corresponds to the set of weights in part  $i$  of Lemma B.5. For example,  $B_2 = \mathcal{W}_0^+(1)$  and  $B_8 = \bigcup_{i \in \mathcal{P}_S \cap \mathcal{P}_J} \mathcal{U}_0^-(i) \cap \mathcal{U}_0^+(1)$ .

Define the following:

$$N_{W_t}^{(1)}(\mathbf{x}) = \sum_{i \in B_2} \max_j \{\sigma(w^{(i)} \cdot \mathbf{x}_j^+)\}$$

$$N_{W_t}^{(2)}(\mathbf{x}) = - \sum_{i \in B_6} \max_j \{\sigma(u^{(i)} \cdot \mathbf{x}_j)\}$$

$$\begin{aligned} N_{W_t}^{(3)}(\mathbf{x}) &= \sum_{i \in B_4} \max_j \{\sigma(\mathbf{w}^{(i)} \cdot \mathbf{x}_j)\} \\ &\quad - \sum_{i \in B_8} \max_j \{\sigma(\mathbf{u}^{(i)} \cdot \mathbf{x}_j)\} \end{aligned}$$

and

$$\begin{aligned} N_{W_t}^{(4)}(\mathbf{x}) &= N_{W_t}(\mathbf{x}) - N_{W_t}^{(1)}(\mathbf{x}) - N_{W_t}^{(2)}(\mathbf{x}) - N_{W_t}^{(3)}(\mathbf{x}) \\ &= \sum_{i \in B_1 \cup B_3} \max_j \{\sigma(\mathbf{w}^{(i)} \cdot \mathbf{x}_j)\} \\ &\quad - \sum_{i \in B_5 \cup B_7} \max_j \{\sigma(\mathbf{u}^{(i)} \cdot \mathbf{x}_j)\} \end{aligned}$$

We would like to analyze the dynamics of  $N_{W_t}(\mathbf{x}^+)$ . To do so, we will address each  $N_{W_t}^{(i)}(\mathbf{x}^+)$  in turn for  $1 \leq t \leq t^*$ .

**Bounding  $N_{W_t}^{(1)}(\mathbf{x}^+)$ :** By Lemma B.5 part 1, it follows that  $N_{W_t}^{(1)}(\mathbf{x}^+) = \sum_{j \in B_2} \mathbf{w}_0^{(j)} + \frac{c_\eta t |B_2|}{2k}$  for all  $1 \leq t \leq t^*$ . Recall the definition of  $\gamma$  in Eq. 17. Then, by Lemma B.2, for sufficiently small  $\epsilon$  and  $k > \text{poly}(\log d, \frac{1}{\epsilon})$  it holds that:

$$\left| \frac{|B_2|}{k} - \gamma \right| \leq \epsilon$$

By Lemma B.4, we have:

$$\left| \sum_{j \in B_2} \mathbf{w}_0^{(j)} \right| \leq |B_2| M \leq (\gamma k + \epsilon k) M$$

Therefore, after  $1 \leq t \leq t^*$  iterations, we have:

$$\left| N_{W_t}^{(1)}(\mathbf{x}^+) - \frac{c_\eta t \gamma}{2} \right| \leq (\gamma k + \epsilon k) M + \frac{c_\eta t \epsilon}{2}$$

By choosing  $M$  and  $\epsilon$  to be sufficiently small (given an upper bound on  $t$  that does not depend on  $M$  and  $\epsilon$ , which we show later),  $\left| N_{W_t}^{(1)}(\mathbf{x}^+) - \frac{c_\eta t \gamma}{2} \right|$  is sufficiently small.

**Calculating  $N_{W_t}^{(2)}(\mathbf{x}^+)$ :** Notice that after  $n - 1$  iterations, we have by Lemma B.5 part 6 that  $N_{W_t}^{(2)}(\mathbf{x}^+) = 0$ . By taking  $c_\eta$  to be sufficiently small, we can ensure that  $n - 1 < t^*$ .

**Bounding  $N_{W_t}^{(3)}(\mathbf{x}^+)$ :** By Lemma B.5 parts 4 and 8 and given that  $M \ll c_\eta$  we have for  $1 \leq t \leq t^*$ :

$$\begin{aligned} N_{W_t}^{(3)}(\mathbf{x}^+) &= \\ &\frac{c_\eta}{2k} \left( \sum_{i \in \mathcal{P}_S \cap \mathcal{P}_J} |\mathcal{W}_0^+(i) \cap \mathcal{W}_0^-(2)| - \sum_{i \in \mathcal{P}_S \cap \mathcal{P}_J} |\mathcal{U}_0^-(i) \cap \mathcal{U}_0^+(1)| \right) \end{aligned}$$

By Lemma B.3, for sufficiently small  $\epsilon$ , for any  $i \in \mathcal{P}_S \cap \mathcal{P}_J$ , the difference

$$\frac{1}{k} (|\mathcal{W}_0^+(i) \cap \mathcal{W}_0^-(2)| - |\mathcal{U}_0^-(i) \cap \mathcal{U}_0^+(1)|)$$

is sufficiently small. We conclude that  $N_{W_t}^{(3)}(\mathbf{x}^+)$  is sufficiently small for small  $\epsilon$ .

**Bounding  $N_{W_t}^{(4)}(\mathbf{x}^+)$ :** By Lemma B.5, parts 1,3,5,7 it follows that

$$N_{W_t}^{(4)}(\mathbf{x}^+) \leq kM$$

and thus can be made sufficiently small for small  $M$ .

**Finishing the proof:** By combining the previous arguments we have

$$N_{W_t}(\mathbf{x}^+) = \frac{c_\eta t \gamma}{2} + \beta^+$$

for  $1 \leq t \leq t^*$ , where  $\beta^+$  is sufficiently small.

By symmetry, we have:

$$-N_{W_t}(\mathbf{x}^-) = \frac{c_\eta t \gamma}{2} + \beta^-$$

for  $1 \leq t \leq t^*$ , where  $\beta^-$  is sufficiently small.

Our goal is to show that gradient converges to a global minimum at  $T = t^*$ . Let

$$t^+ = \arg \min_{t \leq t^*} \left\{ \frac{c_\eta t \gamma}{2} + \beta^+ > 1 \right\}$$

and

$$t^- = \arg \min_{t \leq t^*} \left\{ \frac{c_\eta t \gamma}{2} + \beta^- > 1 \right\}$$

where the minimum is over integral times  $t$ . Notice that  $t^+ \neq t^-$  can only occur when there exists an integer  $r$  such that

$$\left| 1 - \frac{c_\eta r \gamma}{2} \right| \leq 2 \max\{\beta^+, \beta^-\} \quad (18)$$

Choose  $c_\eta$  to be a small number which is not an integral multiple of  $\frac{2}{\gamma}$  (e.g., choose irrational  $c_\eta$ ). Then,  $\max\{\beta^+, \beta^-\}$  can be made sufficiently small such that Eq. 18 does not hold.<sup>7</sup> In this case, after  $\frac{1}{\gamma c_\eta} \leq t^+ = t^- = t^* \leq \frac{3}{\gamma c_\eta}$  iterations, gradient descent converges to a global minimum.  $\square$

### B.3. Finishing the Proof of Theorem 8.1

We are now ready to prove the theorem. Gradient descent converges to a global minimum after  $\frac{1}{\alpha c_\eta} \leq T \leq \frac{3}{\alpha c_\eta}$  iterations by Lemma B.6. Furthermore, by the proof of Lemma B.6,  $\mathcal{W}_T^+(1) = \mathcal{W}_0^+(1)$ . For each  $j \in \mathcal{W}_0^+(1)$ , the norm of  $\mathbf{w}_T^{(j)}$  is at least  $\frac{\eta}{2} T \geq \frac{1}{2\gamma k}$ . Therefore, for a sufficiently small  $\epsilon$  by Lemma B.2:

$$M_{\mathbf{w}}^+(1) \geq \frac{|\mathcal{W}_0^+(1)|}{2\gamma k} \geq \frac{1}{3}$$

Now, by Lemma B.6, for all  $j \notin \mathcal{W}_0^+(1)$ , it holds that  $|\mathbf{w}_T^{(j)}| \leq |\mathbf{w}_0^{(j)}| + \frac{\eta}{2} \leq \eta = \frac{c_\eta}{k}$ . Therefore, for all  $\mathbf{p}_i \in \mathcal{P}_J \cup \mathcal{P}_+$ ,  $M_{\mathbf{w}}^-(i) \leq c_\eta$ . By symmetry, it follows that the PSI property holds with  $b = 1$  and  $c = \sqrt{18}c_\eta$ .

<sup>7</sup>Note that  $\max\{\beta^+, \beta^-\}$  does not depend on  $c_\eta$ .